# Lipoprotein lipase (LpL) on the surface of cardiomyocytes increases lipid uptake and produces a cardiomyopathy

Hiroaki Yagyu,[1] Guangping Chen,[1] Masayoshi Yokoyama,[1] Kumiko Hirata,[1] Ayanna Augustus,[1] Yuko Kako,[1] Toru Seo,[2] Yunying Hu,[1] E. Peer Lutz,[3] Martin Merkel,[3] André Bensadoun,[4] Shunichi Homma,[1] and Ira J. Goldberg[1]

[1]Department of Medicine, Columbia University, New York, New York, USA
[2]Department of Pediatrics and Institute of Human Nutrition, Columbia University, New York, New York, USA
[3]Department of Medicine, University of Hamburg, Hamburg, Germany
[4]Division of Nutritional Sciences, Cornell University, Ithaca, New York, USA

**Lipoprotein lipase is the principal enzyme that hydrolyzes circulating triglycerides and liberates free fatty acids that can be used as energy by cardiac muscle. Although lipoprotein lipase is expressed by and is found on the surface of cardiomyocytes, its transfer to the luminal surface of endothelial cells is thought to be required for lipoprotein lipase actions. To study whether nontransferable lipoprotein lipase has physiological actions, we placed an α-myosin heavy-chain promoter upstream of a human lipoprotein lipase minigene construct with a glycosylphosphatidylinositol anchoring sequence on the carboxyl terminal region. Hearts of transgenic mice expressed the altered lipoprotein lipase, and the protein localized to the surface of cardiomyocytes. Hearts, but not postheparin plasma, of these mice contained human lipoprotein lipase activity. More lipid accumulated in hearts expressing the transgene; the myocytes were enlarged and exhibited abnormal architecture. Hearts of transgenic mice were dilated, and left ventricular systolic function was impaired. Thus, lipoprotein lipase expressed on the surface of cardiomyocytes can increase lipid uptake and produce cardiomyopathy.**

*J. Clin. Invest.* **111**:419–426 (2003). doi:10.1172/JCI200316751.

## Introduction

Lipoprotein lipase (LpL), the primary enzyme that converts lipoprotein triglyceride (TG) to FFAs, has an unusual intercellular itinerary. It is synthesized by parenchymal cells in muscle and adipose tissue, but is thought to be physiologically active only after it transfers to the endothelial cell and then undergoes transcytosis to the luminal surface. This pilgrimage is unusual in that most proteins are transferred from the circulation to the interstitial space. Both LpL and another heparin-binding protein, IL-8 (1), appear to require both proteoglycans and receptors for this process (2).

The dogma that LpL-mediated lipolysis occurs solely within the vascular lumen suggests that the pool of LpL that is found on the surface of myocytes (3) and adipocytes (4) is nonfunctional. In part, this hypothesis assumes that TG-rich lipoproteins do not leave the vascular compartment and directly interact with adipocytes and myocytes. Several recent lines of experimental evidence, however, suggest that this may be incorrect. Remnant lipoproteins have been found within the artery wall (5), and core lipids, cholesteryl ester, and retinyl esters found in lipoproteins are deposited in hearts, muscle, and adipose tissue (6). A more permeable endothelial barrier will allow this to occur, and several factors including cytokines (7) and fatty acids that result from lipolysis itself (8) enhance permeability.

To test whether LpL on the surface of cardiomyocytes can affect lipid delivery, we created a mutated LpL molecule with a cell-attachment glycosylphosphatidylinositol (GPI) anchor (Figure 1). Transfected cells produced active cell surface LpL that was released when the GPI anchor was cleaved. By creating transgenic mice expressing this protein in cardiomyocytes, we show that LpL does not have to be located on endothelial cells to function in vivo. Furthermore, GPI-anchored human LpL ($hLpL^{GPI}$) transgenic mice developed a dilated cardiomyopathy with lipid accumulation within myocytes.

*Received for publication August 26, 2002, and accepted in revised form December 9, 2002.*

**Address correspondence to:** Ira J. Goldberg, Department of Medicine, Columbia University, 630 West 168th Street, New York, New York 10032, USA. Phone: (212) 305-5961; Fax: (212) 305-5384; E-mail: IJG3@columbia.edu.

**Conflict of interest:** The authors have declared that no conflict of interest exists.

**Nonstandard abbreviations used:** lipoprotein lipase (LpL); triglyceride (TG); glycosylphosphatidylinositol (GPI); GPI-anchored human LpL ($hLpL^{GPI}$); decay-accelerating factor (DAF); myosin heavy chain (MHC); Chinese hamster lung (CHL); phosphatidylinositol-specific phospholipase C (PIPLC); fast performance liquid chromatography (FPLC); carnitine palmitoyltransferase 1 (CPT-1); acyl-CoA oxidase (ACO); atrial natriuretic factor (ANF ); heterozygous LpL knockout (*LpL1*); fraction catabolic rate (FCR); wild-type CHL (W-CHL); TGRP, triglyceride rich particles.

## Methods

*GPI-LpL construct*. A PCR-based strategy was used to ligate the DNA sequence encoding the last 37 amino acids of membrane decay accelerating factor (DAF) (9, 10) containing the GPI-anchoring sequence to a human LpL (hLpL) minigene (11) (see Figure 1a). This strategy required the elimination of the LpL termination codon

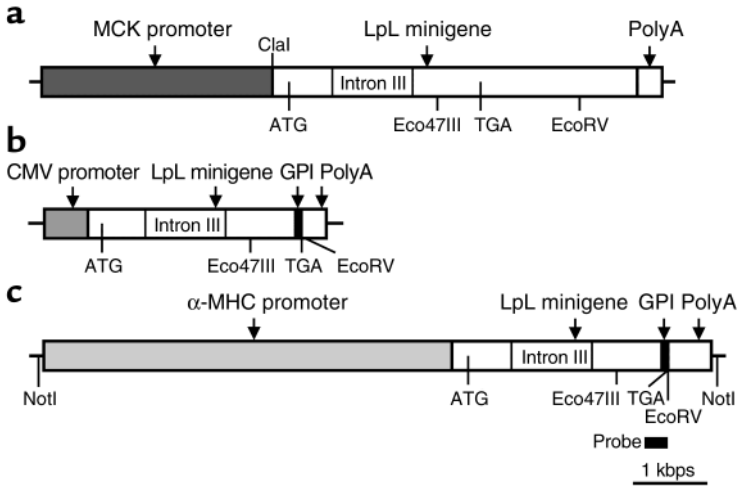


**Figure 1**
The hLpL$^{GPI}$ DNA construction. (**a**) The human LpL minigene with a muscle creatine kinase promoter was used as a template DNA for generating the hLpL$^{GPI}$ DNA construction. The translational start codon (ATG), stop codon (TGA), and the polyadenylation signal (PolyA) are indicated. MCK, muscle creatine kinase. (**b**) The hLpL$^{GPI}$ DNA was inserted into the plasmid containing the CMV promoter for expression in transfected cells. (**c**) The hLpL$^{GPI}$ DNA was subcloned into the plasmid containing the α-MHC promoter. The probe used for Northern blot analysis is indicated. kbps, kilobasepairs.

and the 3′ untranslated region. First, we performed PCR using VENT polymerase (New England Biolabs Inc., Beverly, Massachusetts, USA) with the following primers: sense primer A (5′-AGCGCTCCATTCATCTCTTCA-3′), containing a unique Eco47III restriction site in the downstream region of the hLpL minigene, and antisense primer B (5′-TTCCACTTCCTTTATTTGGGCCTGACTTCTTATTCAGAG-3′). This latter primer contains the first 19 nucleotides in the last 37 amino acids of DAF and the last 20 nucleotides, except the stop codon in the coding region of the hLpL minigene. A 639-bp fragment was produced by primers A and B with hLpL minigene as a template DNA. Second, a complementary primer to B, denoted sense primer C (5′-CTCTGAATAAGAAGTCAGGCCCAAATAAAGGAAGTGGAA-3′) and antisense primer D (5′-GATATCCTAAGTCAGCAAGCCCATGGT-3′), containing an additional EcoRV restriction site and the last 21 nucleotides in the last 37 amino acids of DAF, was used to generate a 140-bp fragment containing the entire coding sequence for the DAF GPI anchoring site by using a plasmid containing DAF cDNA as a template DNA (9). Third, the two PCR products were mixed and amplified using primers A and D to produce a 740-bp fragment containing the LpL Eco47III site, some downstream LpL sequence, and the GPI-anchoring sequence. Fourth, both this fragment and the hLpL minigene were cut with Eco47III and EcoRV, and the fragment was inserted into the minigene.

The modified LpL minigene was subcloned into the plasmid pCMV-Tag2 (Invitrogen Corp., Carlsbad, California, USA) for expression in transfected cells (Figure 1b) and was driven by the cardiac muscle–specific α-myosin heavy chain (MHC) promoter (12) for creation of transgenic mice (Figure 1c).

*Cell transfection*. Chinese hamster lung (CHL) cells were maintained in DMEM supplemented with 10% (vol/vol) FBS and antibiotics. CHL cells were transfected with hLpL$^{GPI}$ DNA by calcium phosphate, selected using G418, and identified by measuring the LpL activity in cell homogenates. LpL activity released with heparin (10 U/ml) and/or phosphatidylinositol-specific phospholipase C (PIPLC; 2 U/ml) for 30 min at 37°C was also measured.

*Transgenic mice*. Transgenic mice were produced that expressed hLpL$^{GPI}$ driven by the α-MHC promoter, and these mice were crossed with heterozygous LpL knockout (*LpL1*) mice (13). A second cross with *LpL1* was used to produce hLpL$^{GPI}$ transgenics on the LpL homozygous knockout mice; this produced *LpL1* littermates with or without the hLpL$^{GPI}$ transgene.

*Lipids, FFA, and glucose*. Blood from fasted (6 h) 2-month-old mice was collected from the retro-orbital plexus. VLDL, IDL/LDL, and HDL were isolated by sequential ultracentrifugation, and fast performance liquid chromatography (FPLC) analyses of plasma lipoproteins were performed as described (14). Two hundred microliters of pooled plasma from 9–11 fasted male mice was subjected to FPLC lipoprotein analyses, and cholesterol content in effluents were measured enzymatically. Cholesterol, TG, FFA, and glucose were measured as described (14). To measure tissue lipids, hearts were rapidly removed and homogenized in ice-cold 1 M NaCl buffer containing protease inhibitors to prevent TG hydrolysis. Lipids were extracted by the Bligh-Dyer method (15) using [$^3$H]cholesterol and 10 μg β-sitosterol as internal standards. Isolated lipids were separated by thin-layer chromatography using the hexanes/diethyl ether/acetic acid (70:30:1) solvent system. Free cholesterol and cholesterol ester masses were determined by gas liquid chromatography as described (16) and were normalized for recovery of [$^3$H]cholesterol and β-sitosterol internal standards. TG and FFA mass were determined by an enzymatic kit as described (17) and were normalized for the recovery of [$^3$H]cholesterol. Experiments were repeated twice using four mice per group in each experiment and showed very similar results.

*LpL activity*. Postheparin plasma was analyzed for LpL activity as described (18). LpL activity in homogenized hearts was measured as described by Hocquette et al. (19). Fasting male mice were injected with heparin (300 U/kg, intravenously). Plasmas were obtained 10 min later and assayed in triplicate for LpL

activity. The contribution of hepatic lipase was determined by assay under high-salt conditions (1 M NaCl final concentration). Human LpL was inhibited using mouse mAb 5D2, which interacts with human, but not mouse, LpL (20).

*Cardiac muscle gene expression*. Tissue RNA (10 μg), isolated using TRIzol reagent (Invitrogen Corp.), was subjected to electrophoresis in 1% agarose gels containing formamide and transferred to nylon filter (Hybond-N; Amersham Pharmacia Biotech Inc., Piscataway, New Jersey, USA). A 448-bp DNA fragment encoding a part of hLpL and GPI anchor (see Figure 1c) radiolabeled with [α-$^{32}$P] deoxy-CTP was used for Northern analysis as reported (21). Heart RNA was also analyzed by Northern blotting using PPARα, carnitine palmitoyltransferase 1 (CPT-1), acyl-CoA oxidase (ACO), atrial natriuretic factor (ANF), GLUT4, and GAPDH probes.

*Lipoprotein uptake*. [$^3$H]VLDL was produced in *LpL1* mice by injection of [$^3$H]palmitate as described (22). Fasted *LpL1* and hLpL$^{GPI}$/*LpL1* mice were injected intravenously via jugular veins with $5.5 \times 10^5$ dpm of [$^3$H]VLDL. Eighty microliters of blood was obtained 0.5, 2, 5, and 15 min after injection. Fifteen minutes after [$^3$H]VLDL injection, mice were perfused with 10 ml of PBS by cardiac puncture. For heparinized animals, heparin (300 U/kg) was injected intraperitoneally 10 min before [$^3$H]VLDL injection. VLDL fraction catabolic rate (FCR) and heart uptake was determined (20).

*Histology*. For immunohistochemistry, hearts of 4-month-old mice were frozen in methylbutane, and LpL was detected as reported (23). Neutral lipids were assessed in hearts from mice fasted for 24 h that were perfused with PBS and embedded in Tissue-Tek OCT compound (Sakura Finetek, Torrance, California, USA). The midventricular slices of myocardium (6-μm thick) were stained with oil red O and counterstained with hematoxylin. Electron microscopy used the left ventricle fixed with 4% glutaraldehyde, postfixed in osmium tetroxide, and embedded in Epon 812. Ultrathin sections were stained with uranyl acetate and lead citrate and examined under JEM-1200ExII electron microscope (JEOL Ltd., Tokyo, Japan).

Frozen heart sections from a 3-month-old *LpL1* and hLpL$^{GPI}$/*LpL1* mouse were used for apoptosis assays. Apoptotic cells were determined by counting TUNEL-positive nuclei (dead-end colorimetric apoptosis detection system; Promega Corp., Madison, Wisconsin, USA).

*Echocardiography*. Two-dimensional echocardiography was performed in conscious 6-month-old female mice using techniques described previously (Sonos 5500 system; Philips Medical Systems, Andover, Massachusetts, USA) (24). Two-dimensional echocardiographic images were obtained and recorded in a digital format. Images were then analyzed off-line by a single observer blinded to the murine genotype (25, 26).

*Statistics*. Data are presented as means ± SD. Student *t* test and ANOVA were used to compare the mean values between two and four groups, respectively. Cumulative survival rates were calculated using Kaplan-Meier survival analysis.

## Results

GPI-LpL expression in CHL cells. We assessed LpL activity in wild-type Chinese hamster lung (W-CHL) and hLpL$^{GPI}$-CHL cells. Both cell lines released little activity spontaneously into the medium (Figure 2). Heparin alone led to no significant increase in activity in the medium; however, PIPLC treatment released LpL activity from hLpL$^{GPI}$-CHL cells (W-CHL versus hLpL$^{GPI}$-CHL, 37 ± 24 versus 172 ± 25 nmol FFA/ml medium/h; $P < 0.01$). The combination of heparin and PIPLC led to the release of even more activity (W-CHL versus hLpL$^{GPI}$-CHL, 61 ± 19 versus 494 ± 4 nmol FFA/ml medium/h; $P < 0.01$).

*Characterization of transgenic mice*. Postheparin plasma was obtained from wild-type and transgenic mice and assayed for LpL activity. Because the effects of additional LpL in previous studies were primarily observed on the LpL-deficient background (20, 27), we crossed these mice onto the *LpL1* background. No increase in postheparin plasma LpL activity was noted (Figure 3a). Moreover, plasmas were incubated with a mAb to human LpL, and no inhibition was noted (data not shown). We then assessed LpL activity in hearts of control (*LpL1*) and transgenic mice. One line of transgenic mice (line 357) showed a marked increase in LpL activity in the heart (Figure 3b), and we studied this line in detail. To assess whether the LpL activity in the heart was from the transgene, i.e., human and not mouse LpL, we used a mAb that does not inhibit mouse LpL (27). As shown in Figure 3c, this Ab inhibited the additional heart LpL; no LpL activity was inhibited in heart muscle homogenates from nontransgenic mice. Northern blot analysis demonstrated high expression of the hLpL$^{GPI}$ transgene only in the heart (Figure 3d).

*Plasma lipids and lipoproteins in mice*. There were no differences in plasma lipids between wild-type and hLpL$^{GPI}$ mice. After crossing the transgene onto the *LpL1* background, male hLpL$^{GPI}$/*LpL1* mice ($n = 11$) had

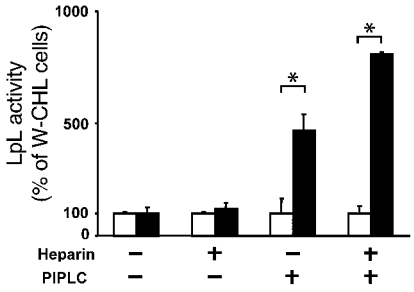


**Figure 2**
LpL activity in the medium. CHL cells were transfected with hLpL$^{GPI}$ DNA. LpL activity in the medium released with heparin (10 U/ml) and/or PIPLC (2 U/ml) for 30 min at 37°C was measured. LpL activity was increased 4.6-fold with PIPLC and 8.1-fold with both PIPLC and heparin in the hLpL$^{GPI}$-CHL cells (black bars), compared with that in W-CHL cells (white bars). Values are expressed as means ± SD. *$P < 0.01$.

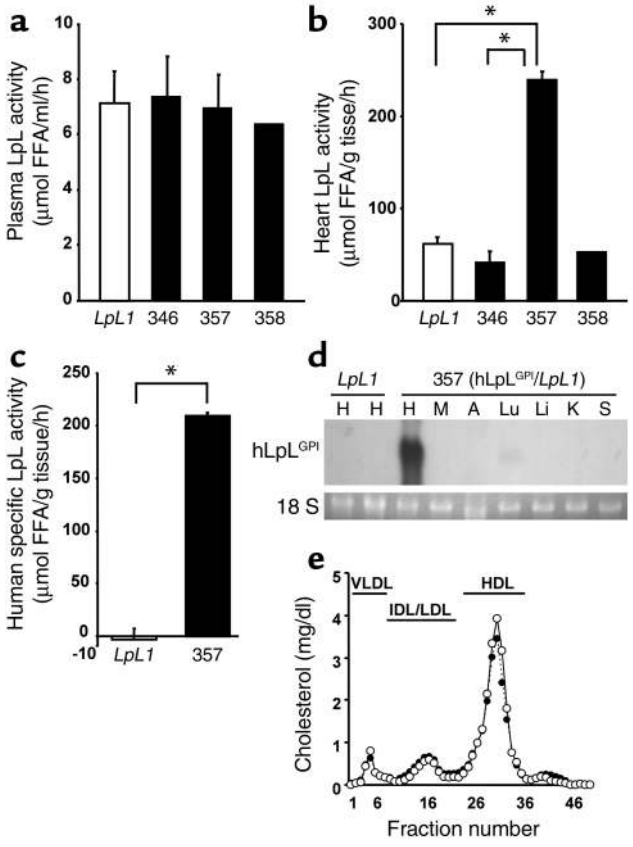


**Figure 3**
LpL expression in plasma and hearts. (**a**) Postheparin plasma LpL activity. There was no difference in postheparin LpL activity between *LpL1* and three lines of hLpL$^{GPI}$/*LpL1* mice. *LpL1*, $n = 6$; line 346, $n = 3$; line 357, $n = 6$; line 358, $n = 2$. (**b**) Heart LpL activity. Hearts from control and three lines of male transgenic animals were homogenized and assayed for LpL activity in triplicate. Homogenates of hearts of hLpL$^{GPI}$/*LpL1* mice (line 357, $n = 3$) had 3.8-fold more LpL activity than control *LpL1* mice ($n = 4$). *$P < 0.01$. (**c**) Myocardial human LpL. Human LpL was differentiated from mouse LpL using an mAb against human LpL activity. All the additional LpL activity in hearts from hLpL$^{GPI}$/*LpL1* mice (line 357, $n = 3$) was inhibited by the Ab, and no inhibition was found when the Ab was added to homogenates from control *LpL1* hearts ($n = 4$). The graph shows the amount of activity inhibited by the Ab. Values are expressed as means ± SD. *$P < 0.01$. (**d**) Northern blot analysis of hLpL$^{GPI}$ mouse tissue RNA. Ten micrograms of total heart RNA from male mice was subjected to Northern blot analysis. Probe is shown in Figure 1c. The hLpL$^{GPI}$ mRNA was detected only in the hearts. H, heart; M, skeletal muscle; A, adipose; Lu, lung; Li, liver; K, kidney; S, spleen. (**e**) Lipoprotein profiles of *LpL1* and hLpL$^{GPI}$/*LpL1* mice. Cholesterol distribution for *LpL1* mice is shown with open circles and hLpL$^{GPI}$/*LpL1* mice with filled circles.

a nonsignificant, 25% lower average TG concentration than *LpL1* mice ($n = 9$) (101 ± 34 mg/dl versus 126 ± 31 mg/dl; $P = 0.10$) due to less VLDL TG (65 ± 27 mg/dl versus 88 ± 26 mg/dl; $P = 0.08$); HDL levels were 39 ± 4 versus 43 ± 5 mg/dl. There were no differences in the elution of LDL or HDL when plasmas were analyzed by FPLC (Figure 3e). There were no lipid differences in female mice (TG; 100 ± 23 mg/dl in eight *LpL1* mice and 97 ± 28 in 13 hLpL$^{GPI}$/*LpL1*; HDL cholesterol was 31 mg/dl in both genotypes). Plasma FFA and glucose levels did not differ between *LpL1* and hLpL$^{GPI}$/*LpL1* mice (data not shown).

When the transgene was bred onto the homozygous LpL-deficient mice, it did not prevent the neonatal demise of these animals; newborn knockout mice still died within 24 h. Thus, the transgene did not provide sufficient intravascular lipolysis to allow knockout mice to survive.

*Lipoprotein kinetic studies*. Plasma clearance of [$^3$H]VLDL did not differ between *LpL1* and hLpL$^{GPI}$/*LpL1* mice (FCR, 13.7 ± 6.6 and 12.1 ± 4.4 pools/h, respectively) (Figure 4a). In the presence of heparin, which normally releases LpL into the bloodstream, the transgene led to a more rapid lipoprotein-TG clearance (FCR, *LpL1* versus hLpL$^{GPI}$/*LpL1* = 15.3 ± 6.0 versus 24.3 ± 7.4 pools/h; $P < 0.02$) (Figure 4b). Thus, the cardiomyocyte anchored LpL added to plasma lipoprotein clearance under these conditions. Hearts of both nonheparinized and heparinized hLpL$^{GPI}$/*LpL1* mice had more lipid uptake than *LpL1* mouse hearts (Figure 4, c and d).

*The hLpL$^{GPI}$ mice have cardiomyopathy*. To determine whether the increased lipid uptake altered heart function, we weighed hearts from *LpL1* and hLpL$^{GPI}$/*LpL1* male and female mice. Hearts weighed 5.2 ± 0.3 mg/g body weight in *LpL1* and 5.7 ± 0.4 mg/g in hLpL$^{GPI}$/*LpL1* mice ($P < 0.01$; Figure 5a).

Male hLpL$^{GPI}$/*LpL1* mice had much greater mortality than *LpL1* mice (Figure 5b). Female mice were primarily used for breeding. During a 32-week breeding period the hLpL$^{GPI}$/*LpL1* mice also had much greater mortality (Figure 5c; cumulative survival, hLpL$^{GPI}$/*LpL1* versus *LpL1* = 0 versus 0.786, $\chi^2 = 7.94$; $P < 0.01$).

Hearts from mice expressing nonmutated human LpL had LpL protein on the surface of cells and in intracellular pools (Figure 6a). As expected, there was intense staining for human LpL protein on the cardiomyocyte surface of hLpL$^{GPI}$ mice (Figure 6b). Oil red O staining showed a marked increase in intracellular neutral lipid in hearts from 24 h–fasted hLpL$^{GPI}$/*LpL1* mice, but not in *LpL1* mice (Figure 6, c and d). Electron microscopy provided further evidence that the hLpL$^{GPI}$ transgene led to a cardiomyopathy. Compared with *LpL1* mice (Figure 6, e and f), the hLpL$^{GPI}$ transgenic hearts had disarrayed cardiomyocyte architecture with increased mitochondria.

Apoptosis in control and hLpL$^{GPI}$/*LpL1* mice was assessed by TUNEL assay. A small number of TUNEL-positive cells were identified in both strains of mice, but there was no difference (data not shown).

To understand the etiology of the cardiac dysfunction, we assessed lipids and gene expression in these hearts. There was no change in TG content (0.67 ± 0.11 μg/mg heart weight in *LpL1* versus 0.69 ± 0.23 μg/mg in hLpL$^{GPI}$/*LpL1*; $P = 0.9$). We observed, however, a 58.9% increase in cholesteryl ester (0.40 ± 0.07 versus

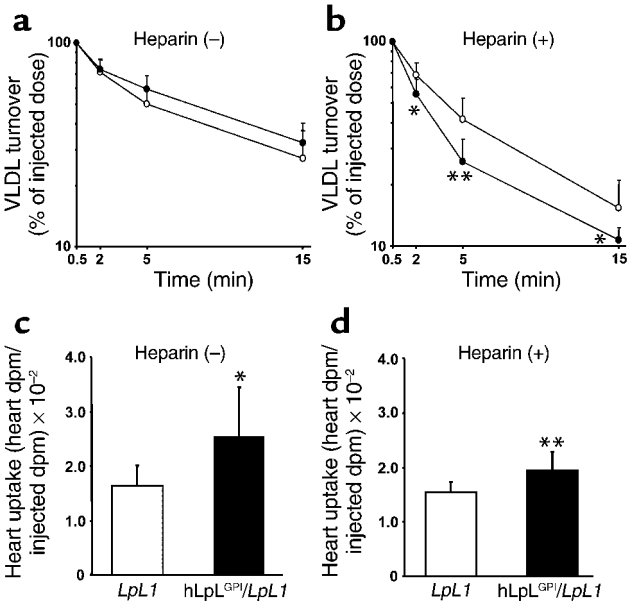


**Figure 4**
VLDL turnover studies in hLpL$^{GPI}$/*LpL1* mice. (**a** and **b**) Plasma VLDL clearance without (**a**) and after heparin injection (**b**) in *LpL1* and hLpL$^{GPI}$/*LpL1* mice. [$^3$H]palmitate-labeled VLDL produced in *LpL1* mice was intravenously injected into *LpL1* and hLpL$^{GPI}$/*LpL1* male mice, and plasma was obtained by retro-orbital bleeds. The plasma count at 0.5 min after injection was considered as the injected dose. Plasma VLDL clearance did not differ between *LpL1* (open circles, $n$ = 9) and hLpL$^{GPI}$/*LpL1* mice (filled circles, $n$ = 8). For FCR, *LpL1* versus hLpL$^{GPI}$/*LpL1* = 13.7 ± 6.6 versus 12.1 ± 4.4 pools/h. Heparinized hLpL$^{GPI}$/*LpL1* mice (filled circles, $n$ = 10) had faster clearance of radiolabeled VLDL than *LpL1* mice (open circles, $n$ = 9). For FCR, *LpL1* versus hLpL$^{GPI}$/*LpL1* 15.3 ± 6.0 versus 24.3 ± 7.4 pools/h, $P < 0.02$. (**c** and **d**) Heart uptake of VLDL-TG (**c**) and after heparin (**d**) from *LpL1* and hLpL$^{GPI}$/*LpL1* mice. (**c**) Hearts of hLpL$^{GPI}$/*LpL1* (black bar, $n$ = 8) mice had 54% more VLDL-TG uptake than control (*LpL1*) hearts (white bar, $n$ = 9). *LpL1* versus hLpL$^{GPI}$/*LpL1* = 0.016 ± 0.004 versus 0.025 ± 0.009 (heart dpm/injected dpm). (**d**) In the presence of heparin, hLpL$^{GPI}$/*LpL1* mice (black bar, $n$ = 10) had 26% more VLDL-TG uptake in the hearts compared with control *LpL1* mice (white bar, $n$ = 9). *LpL1* versus hLpL$^{GPI}$/*LpL1* = 0.015 ± 0.002 versus 0.019 ± 0.003 (heart dpm/injected dpm). Values are expressed as means ± SD. *$P < 0.05$; **$P < 0.01$.

0.63 ± 0.12; $P < 0.05$) and a 24.7% increase in FFA (125.3 ± 29.2 μmol/mg in *LpL1* versus 156.2 ± 24.7 μmol/mg; $P < 0.05$ in hLpL$^{GPI}$/*LpL1* mice).

Several genes that relate to cardiac energetics were assessed by Northern blot analysis. PPARα, CPT-1, and ACO were increased (Figure 6g). ANF, a heart failure gene, was also stimulated. GLUT4 expression was decreased.

*Echocardiography*. The left ventricles of hLpL$^{GPI}$/*LpL1* mice were significantly dilated, compared with those from *LpL1* mice (Table 1, Figure 7). The left ventricular systolic function of hLpL$^{GPI}$/*LpL1* mice was also significantly impaired. There was no increase in ventricular wall thickness, however.

## Discussion

We created a transgenic mouse expressing hLpL$^{GPI}$, and using this mouse we made several observations. (a) The hLpL$^{GPI}$ transgene led to large amounts of LpL activity in heart homogenates, but no active LpL was released into the bloodstream of heparinized mice. (b) Immunohistochemical studies showed large amounts of LpL protein on the surface of the myocytes. (c) Unlike heart expression of nonanchored LpL (28), the hLpL$^{GPI}$ transgene led to minor changes in plasma lipoproteins and did not prevent the neonatal demise of LpL knockout mice. (d) Nonetheless, cardiac uptake of lipid from circulating lipoproteins was increased in the hLpL$^{GPI}$/*LpL1* mice; heart uptake was also increased in heparinized hLpL$^{GPI}$/*LpL1* mice. (e) hLpL$^{GPI}$-expressing mice had larger hearts and reduced survival after breeding. (f) Hearts of hLpL$^{GPI}$ mice had increased intracellular lipid, disordered cellular structure, and dilated cardiomyopathy.

Myocytes synthesize native LpL, which is then transferred to the luminal surface of capillary endothelial cells (Figure 8). Although some LpL is present on the surface of myocytes and adipocytes, it is generally thought that this represents a nonphysiologically active pool of

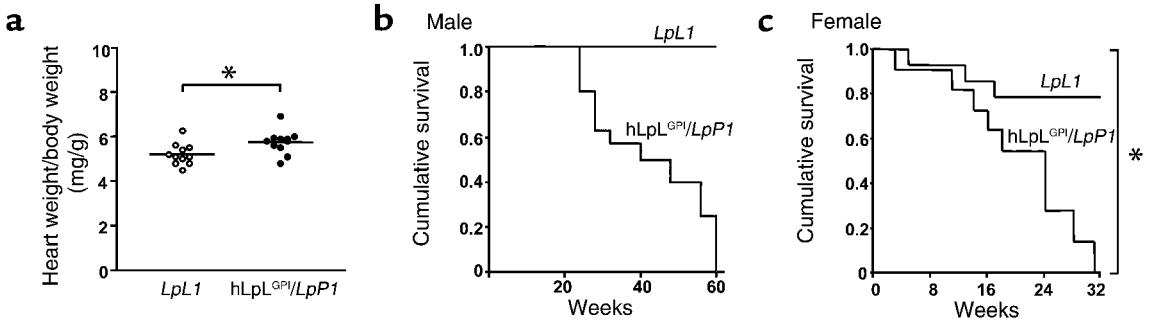


**Figure 5**
Evidence for cardiomyopathy. (**a**) Heart size. Hearts were obtained from 4-month-old male mice, and the heart weight was divided by total body weight. The hLpL$^{GPI}$/*LpL1* mice (filled circles, $n$ = 11) had larger hearts (milligrams per gram body weight) than *LpL1* mice (open circles, $n$ = 11). *$P < 0.02$. (**b** and **c**) Survival. Breeding female hLpL$^{GPI}$/*LpL1* mice ($n$ = 11) died more frequently than *LpL1* female mice ($n$ = 14); males also died more rapidly. The hLpL$^{GPI}$/*LpL1* males ($n$ = 8) also died more rapidly than *LpL1* male mice ($n$ = 14). Differences among survival curves were compared using Kaplan-Meier survival analysis. *$P < 0.01$.

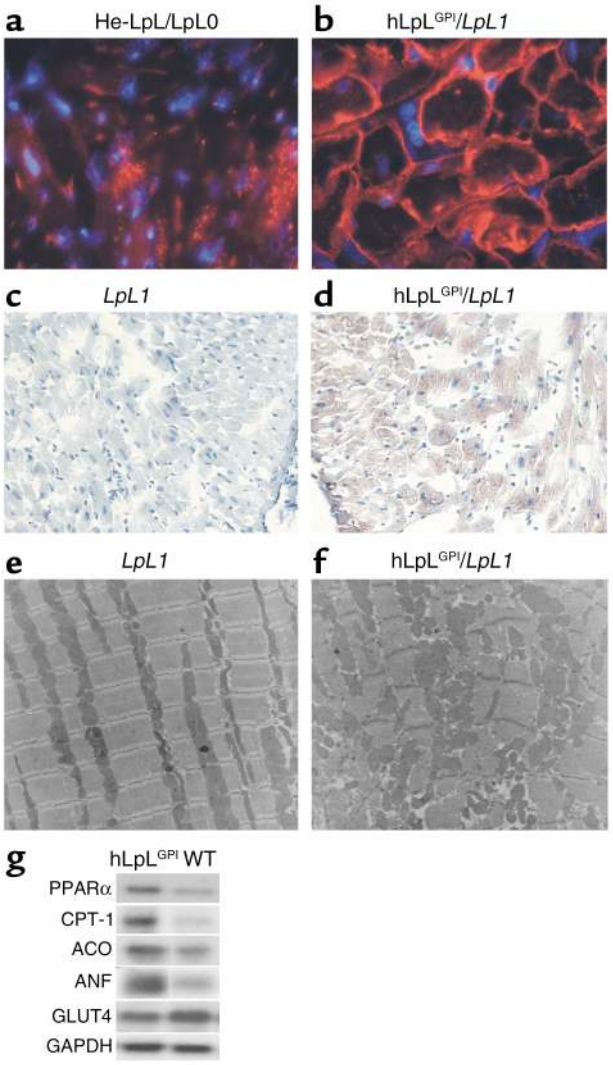


**Figure 6**
(**a** and **b**) LpL immunofluorescence in the hearts. An mAb was used to detect hLpL in hearts. In mice with transgenic expression of normal hLpL in the hearts on the homozygous LpL knockout background (He-LpL/LpL0) (28), hLpL was found in the cytoplasm and at the membrane. Hearts from hLpL$^{GPI}$/*LpL1* mice had intense staining for LpL on the surface of cardiomyocytes. In **a**, intensity of red staining is amplified tenfold compared with **b**. (**c** and **d**) Myocardial lipid accumulation in 24 h–fasted hLpL$^{GPI}$/*LpL1* mice. Oil red O staining shows an abundance of neutral lipid droplets within the cardiomyocytes of hLpL$^{GPI}$/*LpL1* (**d**) mice compared with *LpL1* (**c**) mice. ×400. (**e** and **f**) Electron microscopy. Ultrastructure of *LpL1* mouse myocardial tissues exhibited normal morphological features with well-organized myofilaments and mitochondria (**e**). T tubules are not visible. The hLpL$^{GPI}$/*LpL1* myocytes appeared severely distorted due to more mitochondria, irregular Z band of myofibrils, and dilated T tubules (**f**). (**g**) Northern blot analysis. Ten micrograms of total RNA were isolated from heart and subjected to Northern blot analysis using a part of cDNA encoding PPARα, CPT-1, ACO, ANF, and GLUT4 as probes. GAPDH is shown as a control for loading.

enzyme. We created a construct in which LpL was anchored to the cell surface via a GPI anchor and showed in vitro that this construct produced active LpL. This mode of cell surface attachment was chosen because previous studies (29) had shown that a similar enzyme, hepatic lipase, was active while anchored to the cell surface via a GPI anchor. We are confident that the physiological effects of our transgene were due to myocyte cell surface LpL, and not LpL that dissociated from the cells, for several reasons: First, we found no active human LpL in the postheparin plasma of the transgenic mice despite a robust expression of activity within the heart. Second, unlike expression of nonanchored LpL, our transgene did not appreciably affect plasma lipoproteins and did not prevent the neonatal demise of LpL knockout mice. Thus, the hLpL$^{GPI}$ transgene was unable to hydrolyze large, nascent triglyceride-rich lipoproteins created during nursing. Third, even in the presence of heparin, a condition that releases endothelial cell–associated LpL, the hLpL$^{GPI}$ transgene increased uptake of circulating triglyceride into the heart.

Our data demonstrate that myocyte-associated LpL leads to increased lipid uptake. This finding indicated that either nonlipolyzed or partially lipolyzed particles crossed the endothelial lining of the cardiac vessels and interacted with myocyte-anchored LpL. Although data obtained more than three decades ago showed that peripheral tissues accumulate chylomicron retinyl ester, a core lipid (30), there was widespread belief that that TG lipolysis to fatty acids occurred only in capillaries and that nonhydrolyzable remnant core lipids were cleared by the liver (31). Hultin et al. (32), however, found significant uptake of core lipid from TG-rich particles into the heart and other tissues. Additionally, as shown microscopically in arteries (5), remnants can cross the endothelial barrier either due to their smaller size or because lipolysis products compromise the integrity of the endothelium (8). Thus, TG hydrolysis might not occur exclusively in the vasculature.

Immunohistological studies of hearts (3) and adipose tissue (4) have consistently shown LpL protein on the surface of myocytes and adipocytes. Moreover, adipocytes grown in culture have a significant amount

**Table 1**
Echocardiographic assessment of left ventricular geometry and systolic function in hLpL$^{GPI}$/*LpL1* 357 transgenic line

| | *n* | LVDd (mm) | LVDs (mm) | FS (%) | EDA (cm$^2$) | ESA (cm$^2$) | FAC (%) | WT (mm) |
|---|---|---|---|---|---|---|---|---|
| *LpL1* | 6 | 26.47 ± 1.51 | 11.08 ± 1.53 | 0.58 ± 0.04 | 0.51 ± 0.07 | 0.10 ± 0.03 | 0.80 ± 0.05 | 10.0 ± 1.40 |
| hLpL$^{GPI}$/*LpL1* | 7 | 32.14 ± 2.37$^A$ | 21.44 ± 4.35$^A$ | 0.33 ± 0.12$^A$ | 0.72 ± 0.08$^A$ | 0.27 ± 0.09$^A$ | 0.63 ± 0.10$^A$ | 9.8 ± 1.0 |

LVDd, left ventricular diastolic dimension; LVDs, left ventricular systolic dimension; FS, fractional shortening [(LVDd-LVDs)/LVDd]; EDA, end-diastolic area; ESA, end-systolic area; FAC, fractional area change [(EDA-ESA)/EDA]; WT, anterior wall thickness. $^A P < 0.01$.

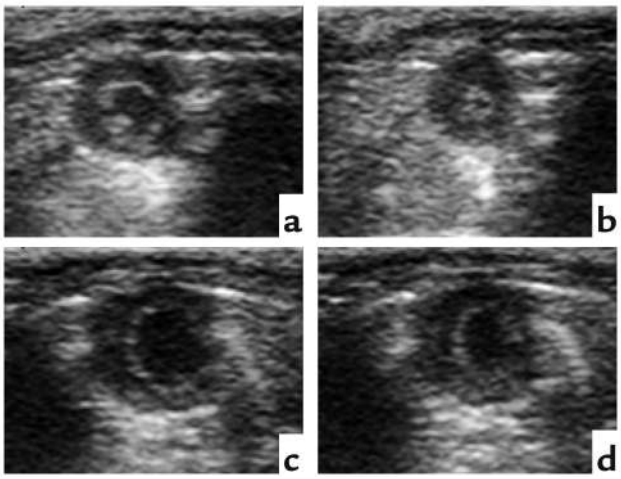


**Figure 7**
Two-dimensional echocardiogram. Representative echocardiographic images from *LpL1* (**a** and **b**) and hLpL$^{GPI}$/*LpL1* (**c** and **d**) mice at end-diastole (left; **a** and **c**) and end-systole (right; **b** and **d**). The left ventricles of hLpL$^{GPI}$/*LpL1* 6-month-old female mice were significantly larger than control *LpL1* mice (see Table 1).

of LpL on the cell surface (33). By creating mutant LpL that was bound to the surface of cardiomyocytes, we showed that LpL is functional at this site. We cannot, however, determine whether cardiomyocyte LpL requires initial lipolysis of nascent circulating lipoproteins. Although increased cardiac TG uptake was found in heparinized transgenic mice, circulating LpL in postheparin blood would initiate lipolysis of injected VLDL. The increased intravascular lipolysis in heparinized mice may have allowed more remnant lipoproteins to interact with the hLpL$^{GPI}$. The more rapid VLDL FCR found after heparinization might have resulted if more VLDL interacted with LpL$^{GPI}$ within the subendothelial space and the partially lipolyzed particles reentered the circulation and were cleared more rapidly in the liver. We also cannot differentiate whether the greater lipid uptake in the hLpL$^{GPI}$ was due to lipolytic functions of the enzyme versus "bridging" functions that increase lipoprotein interaction with the cell surface (23, 34, 35). Nonetheless, our data suggest a novel pathway for cardiac fuel acquisition, cardiomyocyte LpL interaction with lipoproteins.

A second indication that the cardiomyocyte LpL was active was the unexpected development of cardiomyopathy in our mice. We have also observed dilated cardiomyopathy by echocardiography in another independent line of mice that had robust expression of the hLpL$^{GPI}$ transgene (line 345). This was surprising because two other transgenic mice overexpressing LpL in hearts did not have cardiomyopathy (11, 28). In these other situations the heart lipotoxicity may have been prevented by heart secretion of apoB-containing lipoproteins (17, 36). Alternatively, endothelial-associated LpL may primarily modulate plasma lipoprotein levels, whereas cardiomyocyte LpL$^{GPI}$ more effectively increases lipid uptake, as has been conclusively shown to occur in vitro (35).

Excess lipid uptake by hearts might occur in the setting of diabetes mellitus and has been inferred to play a role in development of diabetic cardiomyopathy (37). Obese Zucker rats also develop a cardiac lipotoxicity that might result from abnormalities in lipid uptake or oxidation due to defective leptin actions (38), this might be analogous to the dilated cardiomyopathy seen with obesity (39). Lipid-induced cardiotoxicity occurs in mice overexpressing fatty acyl CoA synthetase (40) and PPAR$\alpha$ (37). The development of cardiomyopathy in the hLpL$^{GPI}$ transgenic mice conclusively demonstrates that excess cardiac lipid uptake, in addition to defective intracellular lipid metabolism, leads to cardiomyopathy. In contrast to these other models, however, we found an increased cardiac content of fatty acids and cholesteryl ester, but not stored TG. This observation, coupled with the induction of several fatty acid–metabolizing genes (CPT-1 and ACO), suggests that excess lipid oxidation is toxic. It is possible that induction of these genes might be a protective response; the cells may be attempting to maximally oxidize toxic lipid intermediates. We expect that future studies in this model and those produced by others will more precisely define the pathophysiology of cardiac lipotoxicity.

In summary, to test the hypothesis that LpL anchored to the surface of parenchymal cells was functional in vivo, we created transgenic mice in which the LpL was expressed and anchored to the myocyte surface. This LpL increased TG uptake by hearts and created a new model of cardiomyopathy. By so doing, we

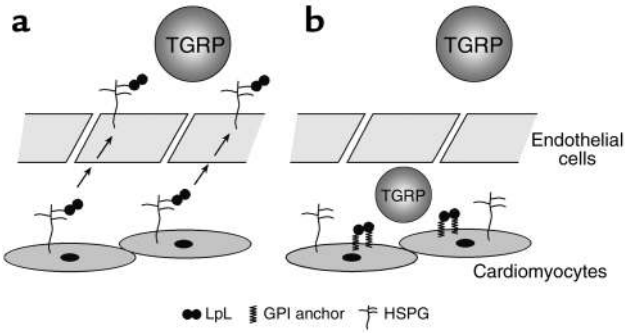


**Figure 8**
Mechanisms of LpL mediated lipid uptake from TG-rich particles in the heart. (**a**) Cardiomyocytes express LpL that dissociates from the cell surface and migrates to the luminal surface of capillary endothelial cells. At this location, LpL attaches to heparan sulfate proteoglycans (HSPG) and is able to interact with circulating TGRP. FFAs are released that cross the endothelial barrier and are acquired by myocytes. (**b**) Our studies show that LpL associated with the cardiomyocyte surface, in this case via a GPI anchor, also promotes lipid uptake. For this to occur, some TGRP, perhaps lipoproteins that are partially digested by endothelial-associated LpL, must exit the vasculature, enter the subendothelial space, and directly interact with cardiomyocytes. It should be noted that LpL is found on both endothelial and cardiomyocyte surfaces. Thus, the LpL-mediated interactions shown in both **a** and **b** are likely to occur in the hLpL$^{GPI}$ mice and may play a role in normal physiology.

demonstrated that myocyte cell surface LpL, as well as LpL on the luminal endothelial surface, is physiologically significant and may contribute to cardiac energetics and, in some circumstances, cardiotoxicity.


## Acknowledgments

This work was supported by grant HL45095 from the National Heart, Lung, and Blood Institute. H. Yagyu was supported in part by a grant from the Japan Health Science Foundation.



1. Middleton, J., et al. 1997. Transcytosis and surface presentation of IL-8 by venular endothelial cells. *Cell.* **91**:385–395.
2. Obunike, J.C., et al. 2001. Transcytosis of lipoprotein lipase across cultured endothelial cells requires both heparan sulfate proteoglycans and the very low density lipoprotein receptor. *J. Biol. Chem.* **276**:8934–8941.
3. Blanchette-Mackie, E.J., Masuno, H., Dwyer, N.K., Olivecrona, T., and Scow, R.O. 1989. Lipoprotein lipase in myocytes and capillary endothelium of heart: immunocytochemical study. *Am. J. Physiol.* **256**:E818–E828.
4. Jonasson, L., Hansson, G.K., Bondjers, G., Bengtsson, G., and Olivecrona, T. 1984. Immunohistochemical localization of lipoprotein lipase in human adipose tissue. *Atherosclerosis.* **51**:313–326.
5. Mamo, J.C., Proctor, S.D., and Smith, D. 1998. Retention of chylomicron remnants by arterial tissue; importance of an efficient clearance mechanism from plasma. *Atherosclerosis.* **141**(Suppl 1**)**:S63–S69.
6. van Bennekum, A.M., et al. 1999. Lipoprotein lipase expression level influences tissue clearance of chylomicron retinyl ester. *J. Lipid Res.* **40**:565–574.
7. Toborek, M., et al. 1996. Linoleic acid and TNF-alpha cross-amplify oxidative injury and dysfunction of endothelial cells. *J. Lipid Res.* **37**:123–135.
8. Rutledge, J., Woo, M., Rezai, A., Curtiss, L., and Goldberg, I. 1997. Lipoprotein lipase increases lipoprotein binding to the artery wall and increases endothelial layer permeability by formation of lipolysis products. *Circ. Res.* **80**:819–828.
9. Caras, I.W., Weddell, G.N., Davitz, M.A., Nussenzweig, V., and Martin, D.W., Jr. 1987. Signal for attachment of a phospholipid membrane anchor in decay accelerating factor. *Science.* **238**:1280–1283.
10. Caras, I.W., et al. 1987. Cloning of decay-accelerating factor suggests novel use of splicing to generate two proteins. *Nature.* **325**:545–549.
11. Levak-Frank, S., et al. 1995. Muscle-specific overexpression of lipoprotein lipase causes a severe myopathy characterized by proliferation of mitochondria and peroxisomes in transgenic mice. *J. Clin. Invest.* **96**:976–986.
12. Kubota, T., et al. 1997. Dilated cardiomyopathy in transgenic mice with cardiac-specific overexpression of tumor necrosis factor-alpha. *Circ. Res.* **81**:627–635.
13. Weinstock, P.H., et al. 1995. Severe hypertriglyceridemia, reduced high density lipoprotein, and neonatal death in lipoprotein lipase knockout mice. Mild hypertriglyceridemia with impaired very low density lipoprotein clearance in heterozygotes. *J. Clin. Invest.* **96**:2555–2568.
14. Yagyu, H., et al. 2002. Very low density lipoprotein (VLDL) receptor-deficient mice have reduced lipoprotein lipase activity. Possible causes of hypertriglyceridemia and reduced body mass with VLDL receptor deficiency. *J. Biol. Chem.* **277**:10037–10043.
15. Bligh, E.A., and Dye, W.J. 1959. A rapid method of total lipid extraction and purification. *Can. J. Biochem. Physiol.* **37**:911–917.
16. Seo, T., et al. 2000. Lipoprotein lipase-mediated selective uptake from low density lipoprotein requires cell surface proteoglycans and is independent of scavenger receptor class B type 1. *J. Biol. Chem.* **275**:30355–30362.
17. Nielsen, L.B., Bartels, E.D., and Bollano, E. 2002. Overexpression of apolipoprotein B in the heart impedes cardiac triglyceride accumulation and development of cardiac dysfunction in diabetic mice. *J. Biol. Chem.* **277**:27014–27020.
18. Lutz, E.P., et al. 2001. Heparin-binding defective lipoprotein lipase is unstable and causes abnormalities in lipid delivery to tissues. *J. Clin. Invest.* **107**:1183–1192.
19. Hocquette, J.F., Graulet, B., and Olivecrona, T. 1998. Lipoprotein lipase activity and mRNA levels in bovine tissues. *Comp. Biochem. Physiol. B Biochem. Mol. Biol.* **121**:201–212.
20. Merkel, M., et al. 1998. Catalytically inactive lipoprotein lipase expression in muscle of transgenic mice increases very low density lipoprotein uptake: direct evidence that lipoprotein lipase bridging occurs in vivo. *Proc. Natl. Acad. Sci. USA.* **95**:13841–13846.
21. Yagyu, H., et al. 2000. Absence of ACAT-1 attenuates atherosclerosis but causes dry eye and cutaneous xanthomatosis in mice with congenital hyperlipidemia. *J. Biol. Chem.* **275**:21324–21330.
22. Aalto-Setala, K., et al. 1992. Mechanism of hypertriglyceridemia in human apolipoprotein (apo) CIII transgenic mice. Diminished very low density lipoprotein fractional catabolic rate associated with increased apo CIII and reduced apo E on the particles. *J. Clin. Invest.* **90**:1889–1900.
23. Merkel, M., et al. 2002. Inactive lipoprotein lipase (LPL) alone increases selective cholesterol ester uptake in vivo, whereas in the presence of active LPL it also increases triglyceride hydrolysis and whole particle lipoprotein uptake. *J. Biol. Chem.* **277**:7405–7411.
24. Takuma, S., et al. 2001. Anesthetic inhibition in ischemic and nonischemic murine heart: comparison with conscious echocardiographic approach. *Am. J. Physiol. Heart Circ. Physiol.* **280**:H2364–H2370.
25. Kocher, A.A., et al. 2001. Neovascularization of ischemic myocardium by human bone-marrow-derived angioblasts prevents cardiomyocyte apoptosis, reduces remodeling and improves cardiac function. *Nat. Med.* **7**:430–436.
26. Wang, C.Y., et al. 2002. Suppression of murine cardiac allograft arteriopathy by long-term blockade of CD40-CD154 interactions. *Circulation.* **105**:1609–1614.
27. Merkel, M., et al. 1998. Lipoprotein lipase expression exclusively in liver. A mouse model for metabolism in the neonatal period and during cachexia. *J. Clin. Invest.* **102**:893–901.
28. Levak-Frank, S., et al. 1999. Induced mutant mouse lines that express lipoprotein lipase in cardiac muscle, but not in skeletal muscle and adipose tissue, have normal plasma triglyceride and high-density lipoprotein-cholesterol levels. *Proc. Natl. Acad. Sci. USA.* **96**:3165–3170.
29. Komaromy, M., Azhar, S., and Cooper, A.D. 1996. Chinese hamster ovary cells expressing a cell surface-anchored form of hepatic lipase. Characterization of low density lipoprotein and chylomicron remnant uptake and selective uptake of high density lipoprotein-cholesteryl ester. *Biochem. Biophys. Res. Commun.* **271**:16906–16914.
30. Goodman, D.S., Stein, O., Halperin, G., and Stein, Y. 1983. The divergent metabolic fate of ether analogs of cholesteryl and retinyl esters after injection in lymph chylomicrons into rats. *Biochim. Biophys. Acta.* **750**:223–230.
31. Cooper, A.D. 1997. Hepatic uptake of chylomicron remnants. *J. Lipid Res.* **38**:2173–2192.
32. Hultin, M., Carneheim, C., Rosenqvist, K., and Olivecrona, T. 1995. Intravenous lipid emulsions: removal mechanisms as compared to chylomicrons. *J. Lipid Res.* **36**:2174–2184.
33. Kern, P.A., Mandic, A., and Eckel, R.H. 1987. Regulation of lipoprotein lipase by glucose in primary cultures of isolated human adipocytes. Relevance to hypertriglyceridemia of diabetes. *Diabetes.* **36**:1238–1245.
34. Williams, K.J., et al. 1992. Mechanisms by which lipoprotein lipase alters cellular metabolism of lipoprotein (a), low density lipoprotein, and nascent lipoproteins. Roles for low density lipoprotein receptors and heparan sulfate proteoglycans. *J. Biol. Chem.* **267**:13284–13292.
35. Goldberg, I.J. 1996. Lipoprotein lipase and lipolysis: central roles in lipoprotein metabolism and atherogenesis. *J. Lipid Res.* **37**:693–707.
36. Boren, J., Veniant, M.M., and Young, S.G. 1998. Apo B100-containing lipoproteins are secreted by the heart. *J. Clin. Invest.* **101**:1197–1202.
37. Finck, B.N., et al. 2002. The cardiac phenotype induced by PPARα overexpression mimics that caused by diabetes mellitus. *J. Clin. Invest.* **109**:121–130. doi:10.1172/JCI200214080.
38. Zhou, Y.T., et al. 2000. Lipotoxic heart disease in obese rats: implications for human obesity. *Proc. Natl. Acad. Sci. USA.* **97**:1784–1789.
39. Kasper, E.K., Hruban, R.H., and Baughman, K.L. 1992. Cardiomyopathy of obesity: a clinicopathologic evaluation of 43 obese patients with heart failure. *Am. J. Cardiol.* **70**:921–924.
40. Chiu, H.C., et al. 2001. A novel mouse model of lipotoxic cardiomyopathy. *J. Clin. Invest.* **107**:813–822.

**Table 1**
Echocardiographic assessment of left ventricular geometry and systolic function in hLpL$^{GPI}$/*LpL1* 357 transgenic line

| | *n* | LVDd (mm) | LVDs (mm) | FS (%) | EDA (cm$^2$) | ESA (cm$^2$) | FAC (%) | WT (mm) |
|---|---|---|---|---|---|---|---|---|
| *LpL1* | 6 | 26.47 ± 1.51 | 11.08 ± 1.53 | 0.58 ± 0.04 | 0.51 ± 0.07 | 0.10 ± 0.03 | 0.80 ± 0.05 | 10.0 ± 1.40 |
| hLpL$^{GPI}$/*LpL1* | 7 | 32.14 ± 2.37$^A$ | 21.44 ± 4.35$^A$ | 0.33 ± 0.12$^A$ | 0.72 ± 0.08$^A$ | 0.27 ± 0.09$^A$ | 0.63 ± 0.10$^A$ | 9.8 ± 1.0 |

LVDd, left ventricular diastolic dimension; LVDs, left ventricular systolic dimension; FS, fractional shortening [(LVDd-LVDs)/LVDd]; EDA, end-diastolic area; ESA, end-systolic area; FAC, fractional area change [(EDA-ESA)/EDA]; WT, anterior wall thickness. $^AP < 0.01$.